

# SDFW Analysis of Mutual Coupling on Microstrip Antenna Array Conformal to Curved

Deepika, Mr. Kapil Mangla, Mr. Umer

**Abstract**— In this paper, Analysis of mutual coupling on microstrip patch antenna array conformal to curved surface is studied for both E-plane and H-plane. Far field radiation patterns and current distributions on individual patches have been obtained and plotted. The effect of E-plane and H-plane separation between radiating elements on mutual coupling coefficients has been analyzed. The approach makes use of the popular and rigorously used spectral domain full wave analysis method in conjunction with method of moment as numerical analysis tool. The electric field due to rectangular patch is obtained by solving integral equation which involves Green's function in spectral domain. The integral equations thus formed are converted into a system of linear equations by the use of method of moment. In the method of moment, the unknown patch current is expressed into a set of linear combination of entire domain basis function weighted by unknown coefficients which are determined after solving linear system of equation. After determining current distribution on the patch antenna, the input impedance and radiation characteristics are obtained. To incorporate the effect of mutual coupling, the scattering matrix is used to describe the multiport network and mutual coupling coefficients are then obtained from scattering parameters. Simulations are done using MATLAB 2007b. Mutual coupling coefficients for E-plane and H-plane coupling are calculated by varying elemental spacing in both E and H-plane.

**Index Terms** — microstrip patch antenna, E-plane, H-plane.

## I. INTRODUCTION

Communication can be broadly defined as the transfer of information from one point to another. The transfer of information within the communication system is commonly achieved by superimposing or modulating the information onto an electromagnetic wave which acts as a carrier for the information signal. At the required destination, the modulated carrier is then received and the original information signal can be recovered by demodulation. Over the years, sophisticated techniques have been developed for this process using electromagnetic carrier waves operating at radio frequencies as well as microwave and millimeter wave frequencies. In today's modern communication industry, antennas are the most important components required to create a communication link.

Deepika, Department of Electronics and Communication Engg. Satya College of Engineering and Technology.

Mr. Kapil Mingle, Assistant Prof., Department of Electronics and Communication Engg. Satya College of Engineering and Technology

Mr. Umer, Asst. Prof. Department of Electronics and Communication Engg. Satya College of Engineering and Technology.

Through the years, Microstrip patch antenna is the most common option used to realize millimeter wave monolithic integrated circuits for microwave, radar and communication purposes [1]. And also, Microstrip antennas have found applications in high performance aircraft, spacecraft, satellite and missiles; where size, weight, cost, performance, ease of installation and aerodynamic profiles are important. Microstrip antennas are most suitable for above mentioned applications because they are low profile, conformable to planar and nonplanar surfaces, simple and easy to manufacture using modern printed circuit technology, mechanically robust when mounted on rigid surfaces, compatible with MIMC design and when the particular patch shape and size are selected; they are very versatile in terms of resonant frequency, polarization, pattern and impedance [2].

Several theoretical models, for the analysis of microstrip antenna have been introduced during the past two decades. Among the first two models were the Transmission line model and Cavity model. Both approaches are relatively easy to implement into a computer program and require relatively short computation time. However, with these models the antenna characteristics are not very accurate and are usually limited to the case of narrow band microstrip antennas [3]. Later more rigorous methods have been proposed such as Full Wave Analysis, FDTD and MPIE. In these methods, the antenna characteristics can be determined by solving the integral equations (method of moment). The integral equation methods are not restricted to the case of single

Microstrip patch antenna but can also be applied to microstrip array and to multilayer configuration. However a major drawback of these methods is long computation time and the relatively large computer memory requirements [4].

## II. ANALYSIS APPROACH

Along with the above mentioned fascinating advantages, microstrip antenna suffers from severe limitations of low bandwidth, efficiency and low gain. When the present research was started in 1981, most microstrip antennas had a bandwidth of only a few percent [5]. The research activities since then have concentrated on developing the bandwidth enhancement techniques for microstrip antennas. The well known techniques for the bandwidth enhancement are either using electrically thick substrates or formation of arrays. However, electrically thick substrates often give rise to an inductive shift in the input impedance, which means that a good impedance match can only be achieved, if a complicated and expensive input network is used [6]. So the array formation technique gives improved results along with enhancement in gain with a little negative effect on the

radiation pattern and the radiation efficiency. However, when two patch elements are brought in the vicinity of each other, the exchange of energy takes place which is termed as mutual coupling. Mutual coupling significantly affects both near field and far field patterns. Thus it is necessary to take into account the effect of mutual coupling while analyzing planar or stacked patch arrays.

In this paper, effect of mutual coupling on rectangular microstrip patch antenna array conformal to cylindrical surface is studied for both E-plane and H-plane. Far field radiation patterns and current distributions on individual patches have been obtained and plotted. The effect of E-plane and H-plane separation between radiating elements on mutual coupling coefficients has been analyzed.

The approach makes use of the popular and rigorously used spectral domain full wave analysis method in conjunction with method of moment as numerical analysis tool. In the analysis, the solution for electric field due to rectangular patch is obtained by solving integral equation which involves Green's function in spectral domain. The Green's function is very strong mathematical tool to solve differential equations subjected to certain boundary conditions [7]. The integral equations thus formed are converted into a system of linear equations by the use of method of moment. In the method of moment, the unknown patch current is expressed into a set of linear combination of basis function weighted by unknown coefficients which are determined by the solution of linear system of equation. To obtain an exact solution for the current distribution on patch antenna the expansion of unknown current distribution has to be an infinite summation and the set of basis function have to form a complete set. But to reduce the complexity of computation, summation is truncated at the maximum value and thus an approximation of the exact solution is obtained. In general, two types of basis functions are used; Entire Domain Basis Function and Sub-Domain Basis Function. However, a major disadvantage of sub-domain basis function is that they require more computation time and computer memory than properly chosen entire domain basis function [8]. The present work thus makes use of entire domain basis functions to expand unknown patch current density. The linear set of equations is solved using MoM to determine unknown patch current. After determining current distribution on the patch antenna, the input impedance and radiation characteristics are obtained. To incorporate the effect of mutual coupling, the scattering matrix related to the direct measurement of incident, reflected, and transmitted waves is used to describe the multiport network problem completely and mutual coupling coefficients are then obtained from scattering parameters.

One of the greatest advantages of microstrip antenna is that it can be conformal to surfaces. Most important conformal antenna structures are spherical, cylindrical and conical [9]. Our study is restricted to conformal microstrip antenna on cylindrical surfaces. Typical geometry of cylindrical antenna is:

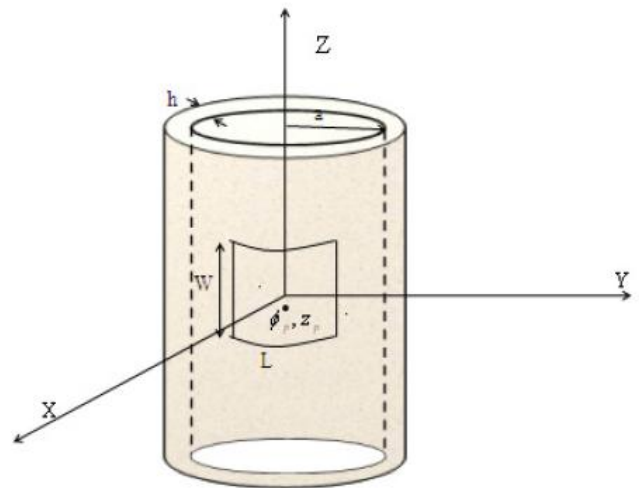


Fig.1: Patch on a curved surface

Full-wave analysis method has been used to analyze such configuration due to following limitations of transmission line model and cavity model:

The models are approximate models and give accurate results only for thin substrates.

Some of the feed configurations such as proximity-coupled and aperture-coupled micro-strip feeds are difficult to model.

Cross-polarized radiation from a patch antenna can't be predicted using the transmission line model because only a single-mode analysis is generally carried out.

Full wave analysis techniques are rigorous and accurate and thus above mentioned limitations can be overcome. Main disadvantage of full-wave solution is that it requires intensive computations. There are three main full-wave analysis techniques:

- Spectral-domain full-wave solution ( uses green's function)
- Mixed-potential electric field integral equation approach (MPIE)
- Finite-difference time-domain technique (FDTD)

### III. ELECTRIC FIELD DUE TO RECTANGULAR PATCH ON CURVED SURFACE

The geometry of rectangular patch on curved surface is depicted in figure.1. The cylinder has been assumed infinite along z-direction. Inner surface of cylinder is perfectly conducting ground plane and a patch having dimensions L and W is probe fed at a point  $(\rho = b, \phi = \phi_p, z = z_p)$ . For the analysis of TM<sub>0n</sub>, the patches are replaced by the surface currents  $J_i(i = x, z)$ . The azimuth component of the current  $J_\phi$  is set to zero because of the high Q value. The total electric field on the patches induced by the patch currents  $J_z$  and the probe-fed current  $J_p$  has been evaluated. At the end of the derivation, the transverse electric field will be expressed as convolutions of the Green's functions.

There are two possible methods to obtain solution for electric field: 1) vector potential method 2) Direct solution of wave equation for  $E_z$  and  $H_z$ . We have employed second approach here because it is comparatively simpler and straightforward.

Electric field and magnetic field at an arbitrary point in a source-free region satisfies

Homogeneous Helmholtz equation, where E denotes electric field in phasor form with time variation ( $e^{j\omega t}$ ) assumed and suppressed.

Since the patch is on cylindrical surface, it would be easier to carry out solution in cylindrical coordinates. The electric field at an arbitrary point, has components in each coordinate.

$$E(\rho, \phi, z) = \hat{a}_\rho E_\rho(\rho, \phi, z) + \hat{a}_\phi E_\phi(\rho, \phi, z) + \hat{a}_z E_z(\rho, \phi, z) \quad \dots (II)$$

So equation (I) is transformed into

$$\nabla^2[\hat{a}_\rho E_\rho + \hat{a}_\phi E_\phi + \hat{a}_z E_z] + \beta^2[\hat{a}_\rho E_\rho + \hat{a}_\phi E_\phi + \hat{a}_z E_z] = 0 \quad \dots (III)$$

The above equation reduces to three scalar partial differential equations

$$\nabla^2 E_\rho + \left(-\frac{E_\rho}{\rho^2} - \frac{2}{\rho^2} \frac{\partial E_\rho}{\partial \phi}\right) = -\beta^2 E_\rho \quad \dots (IV)$$

$$\nabla^2 E_\phi + \left(-\frac{E_\phi}{\rho^2} - \frac{2}{\rho^2} \frac{\partial E_\phi}{\partial \phi}\right) = -\beta^2 E_\phi \quad \dots (V)$$

$$\nabla^2 E_z = -\beta^2 E_z \quad \dots (VI)$$

From above mentioned three scalar equations, first two equations are coupled i.e., each equation has more than one dependent variable. Thus solution is obtained from third differential equation involving E z which is un-coupled and thus easier to solve. In each equation the Laplacian operator in cylindrical coordinate system is given by:

$$\nabla^2 E_z(\rho, \phi, z) = \frac{\partial^2 E_z}{\partial \rho^2} + \frac{1}{\rho} \frac{\partial E_z}{\partial \rho} + \frac{1}{\rho^2} \frac{\partial^2 E_z}{\partial \phi^2} + \frac{\partial^2 E_z}{\partial z^2} \quad \dots (VII)$$

Using variable separation method, the solution of E z is assumed to be product of three functions f, g and h; each of which is respectively function of x, y and z alone.

$$E_z(\rho, \phi, z) = f(\rho)g(\phi)h(z) \quad \dots (VIII)$$

Equation (VI), then, further reduces into three scalar equations in f, g, and h whose solutions can be found easily.

$$\frac{\rho^2 \partial^2 f}{\partial \rho^2} + \rho \frac{\partial f}{\partial \rho} + [(k_\rho \rho)^2 - n^2]f = 0 \quad \dots (IX)$$

$$\frac{\partial^2 g}{\partial \phi^2} = -m^2 g \quad \dots (X)$$

$$\frac{\partial^2 h}{\partial z^2} = -k_z^2 h \quad \dots (XI)$$

Subjected to constraint equation,

The solution is found in three steps: solving wave equation for  $E_z$  and  $H_z$ , taking two dimensional Fourier transform of fields and then calculating the other field components with the help of  $E_z$  and  $H_z$ . The other field components are related to  $E_z$  and  $H_z$  by following relation relations:

$$E_\rho = \frac{j k_z \frac{\partial E_z}{\partial \rho} + \frac{\omega \mu_0 \partial H_z}{\rho \partial \phi}}{k_\rho^2} \quad \dots (XII)$$

$$E_\phi = \frac{j k_z \frac{\partial E_z}{\partial \phi} + \omega \mu_0 \frac{\partial H_z}{\partial \rho}}{k_\rho^2} \quad \dots (XIII)$$

$$H_\rho = \frac{-j \omega \epsilon \frac{\partial E_z}{\partial \rho} + k_z \frac{\partial H_z}{\partial \phi}}{k_\rho^2} \quad \dots (XIV)$$

$$H_\phi = \frac{j \omega \epsilon \frac{\partial E_z}{\partial \phi} + k_z \frac{\partial H_z}{\partial \rho}}{k_\rho^2} \quad \dots (XV)$$

The solution for  $E_z$  and  $H_z$  is assumed such that wave is travelling outside the outer boundary of the cylinder and standing inside the substrate region of geometry. Thus  $E_z$  and  $H_z$  are given as: In region I,  $a < \rho < b$

$$E_z = [A_{1n} H_n^{(1)}(k_{1\rho} \rho) + B_{1n} J_n(k_{1\rho} \rho)] e^{jn\phi} e^{jk_z z} \quad \dots (XVI)$$

$$H_z = [C_{1n} H_n^{(1)}(k_{1\rho} \rho) + D_{1n} J_n(k_{1\rho} \rho)] e^{jn\phi} e^{jk_z z} \quad \dots (XVII)$$

In region II,  $\rho > b$

$$E_{z2} = A_{2n} H_n^{(1)}(k_{1\rho} \rho) e^{jn\phi} e^{jk_z z} \quad \dots (XVIII)$$

$$H_{z2} = C_{2n} H_n^{(1)}(k_{1\rho} \rho) e^{jn\phi} e^{jk_z z} \quad \dots (XIX)$$

#### IV. BOUNDARY CONDITIONS

The field components are subjected to following boundary conditions:

Tangential electric field is zero on inner wall of cylinder i.e. at  $\rho = a$

$$E_{z1} = 0, E_{\phi1} = 0$$

Tangential electric field is continuous on outer wall of cylinder i.e. at  $\rho = b$

$$E_{\phi1} = E_{\phi2}, E_{z1} = E_{z2} \text{ at } \rho = b$$

Where,  $E_{j1}$ ,  $E_{j2}$  and  $E_{z1}$ ,  $E_{z2}$  correspond to j-directed and z-directed electric fields in region-1 and region-2 correspondingly

Region-1  $a < \rho < b$

Region-2  $\rho > b$

Tangential Magnetic field is continuous in z-direction as current distribution is assumed constant in j-direction; while j-directed magnetic field is discontinuous by an amount equal to z-directed surface current density at boundary  $\rho = b$

$$H_{z1} = H_{z2}$$

$$\vec{H}_{\phi1} - \vec{H}_{\phi2} = \vec{J}_z$$

The electric field and magnetic field outside cylinder boundary is thus given by putting value of  $A_{2n}$

$$E_{z2} = -\frac{j \omega \mu_0 b^2 k_{1\rho} k_{2\rho} P(k_{1\rho} b) [Q(k_{1\rho}) k_{2\rho} - R Q(k_{1\rho} b) k_{1\rho}]}{k_0^2 [\epsilon_r b^2 (P(k_{1\rho} b) - R P(k_{1\rho} b))]} \vec{J}_z e^{jn\phi} e^{jk_z z} \quad \dots (XX)$$

V. APPLICATION OF METHOD OF MOMENT

In this section a short summary will be given for the method of moment formulation. The formulation is done in the spectral domain which means that all quantities used are Fourier transformed. The electric field  $E_z$  and its corresponding Fourier transform  $E_z$  are defined as:

$$E_z(\rho, \phi, z) = \sum_{n=-\infty}^{\infty} e^{jn\phi} \int_{-\infty}^{\infty} \tilde{E}_z(\rho, \phi, z) e^{jk_z z} \dots \text{(XXI)}$$

In the moment method formulation the Green's function, due to a point current source located at an arbitrarily point in the dielectric, is needed. Once the Green's function is known, a Galerkin type of moment method can be formulated, which results in the matrix equation:

$$[V] = [Z] [I] \dots \text{(XXII)}$$

By applying boundary condition at the patch metallization associated with the tangential electric field on a highly conducting patch

$$\hat{z} \times \vec{E}_{total} = 0 \dots \text{(XXIII)}$$

The total electric field on the patch induced by the patch current and probe fed current, so that equation (XXIII) can be written as:

$$\hat{z} \times [E(j_s) + E(j_p)] = 0 \dots \text{(XXIV)}$$

As shown in equation (XXIV) tangential electric field is contributed by both excitation current and patch current.

$$\hat{z} \times \left[ \int_{-\infty}^{\infty} \begin{bmatrix} \tilde{G}_{zz} \\ \tilde{G}_{z\phi} \end{bmatrix} [j_s] e^{jk_z z} e^{jk_\phi \phi} dk_z dk_\phi + \int_{-\infty}^{\infty} \begin{bmatrix} \tilde{G}_{zz} & \tilde{G}_{z\phi} \\ \tilde{G}_{\phi z} & \tilde{G}_{\phi\phi} \end{bmatrix} [j_z] e^{jk_z z} e^{jk_\phi \phi} dk_z dk_\phi \right] = 0 \dots \text{(XXV)}$$

Integral equation (XXV) can be solved numerically by applying MoM. The first step in the MoM is the expansion of unknown currents into a set of linear combination of basis function:

$$\begin{bmatrix} j_z \\ j_\phi \end{bmatrix} = \begin{bmatrix} \sum_{m=1}^2 I_{mz} \tilde{j}_{mz} \\ \sum_{n=1}^2 I_{n\phi} \tilde{j}_{n\phi} \end{bmatrix} \dots \text{(XXVI)}$$

Where  $I_{mz}$  and  $I_{nz}$  are the mode coefficients (unknown currents) that have to be determined and  $\tilde{j}_{mz}$  and  $\tilde{j}_{n\phi}$  are the basis function or mode.

By substitute the value of equation (XXVI) in equation (XXIV), Equation (XXIV) can be rewritten as:

$$\hat{z} \times \left[ \int_{-\infty}^{\infty} \begin{bmatrix} \tilde{G}_{zz} \\ \tilde{G}_{z\phi} \end{bmatrix} [j_s] e^{jk_z z} e^{jk_\phi \phi} dk_z dk_\phi + \int_{-\infty}^{\infty} \begin{bmatrix} \tilde{G}_{zz} & \tilde{G}_{z\phi} \\ \tilde{G}_{\phi z} & \tilde{G}_{\phi\phi} \end{bmatrix} \begin{bmatrix} \sum_{m=1}^2 I_{mz} \tilde{j}_{mz} \\ \sum_{n=1}^2 I_{n\phi} \tilde{j}_{n\phi} \end{bmatrix} e^{jk_z z} e^{jk_\phi \phi} dk_z dk_\phi \right] = 0 \dots \text{(XXVII)}$$

Applying Galerkin's procedure i.e. taking inner product with test function (identical to basis function):

$$\hat{z} \times \left[ \int_{-\infty}^{\infty} \begin{bmatrix} \tilde{G}_{zz} \\ \tilde{G}_{z\phi} \end{bmatrix} \tilde{j}_{test} [j_s] e^{jk_z z} e^{jk_\phi \phi} dk_z dk_\phi + \int_{-\infty}^{\infty} \begin{bmatrix} \tilde{G}_{zz} & \tilde{G}_{z\phi} \\ \tilde{G}_{\phi z} & \tilde{G}_{\phi\phi} \end{bmatrix} \begin{bmatrix} \sum_{m=1}^2 I_{mz} \tilde{j}_{mz} \\ \sum_{n=1}^2 I_{n\phi} \tilde{j}_{n\phi} \end{bmatrix} \tilde{j}_{test} e^{jk_z z} e^{jk_\phi \phi} dk_z dk_\phi \right] = 0 \dots \text{(XXVIII)}$$

Which, can be written as

$$\begin{bmatrix} [V_{mz}]_{m=1,2,\dots,M} \\ [V_{n\phi}]_{n=1,2,\dots,N} \end{bmatrix} = \begin{bmatrix} Z_{zz}^{mn} & Z_{z\phi}^{mn} \\ Z_{\phi z}^{mn} & Z_{\phi\phi}^{mn} \end{bmatrix} \begin{bmatrix} [I_{mz}]_{m=1,2,\dots,M} \\ [I_{n\phi}]_{n=1,2,\dots,N} \end{bmatrix} \dots \text{(XXIX)}$$

Voltage Vector Impedance Matrix Excitation Vector

The matrix  $[Z]$  contain  $N * N$  element and  $[I]$  is a vector containing  $N$  unknown mode coefficients, and  $[V]$  is the excitation vector containing  $N$  element.

The entries in the impedance matrix are specified as given by the expression

$$Z_{ij}^{mn} = \int_{-\infty}^{\infty} \int_{-\infty}^{\infty} \tilde{G}_{ij} \tilde{j}_{mi} \tilde{j}_{nj} e^{jk_z z} e^{jk_\phi \phi} dk_z dk_\phi$$

$$V_{mi} = \int_{-\infty}^{\infty} \int_{-\infty}^{\infty} \tilde{G}_{\phi i} \tilde{j}_{mi} \tilde{j}_s e^{jk_z z} e^{jk_\phi \phi} dk_z dk_\phi$$

VI. MUTUAL COUPLING EFFECT IN CURVED ARRAY

When two patch elements are brought in the vicinity of each other, the current in each element changes in both amplitude and phase. The amount of change depends on the mutual coupling between the elements. Since the currents are changed, the far-fields due to these elements change. To find the resultant far-field radiation pattern, the variation in the phase and amplitude of the currents in these two individual patch elements are calculated first and then the resultant far-field pattern can be found. Self and mutual impedances can be derived from the near field calculations. These impedance expressions can be used to find the effective current distributions on the individual patch elements. The current distributions are then used for calculating the far field which is the required field in the presence of mutual coupling.

In present study, an array of two horizontal patches on cylindrical surfaces is considered. The two patches are considered of same size.



To study mutual coupling for an array of two patches, the two probe-fed micro-strip antennas are treated as a two-port network with a 2\*2 port matrix [Z]. The relation between the port voltages and currents are defined as

$$\begin{bmatrix} V^1 \\ V^2 \end{bmatrix} = \begin{bmatrix} Z^{11} & Z^{12} \\ Z^{21} & Z^{22} \end{bmatrix} \begin{bmatrix} I_1 \\ I_2 \end{bmatrix} \quad \dots (xxx)$$

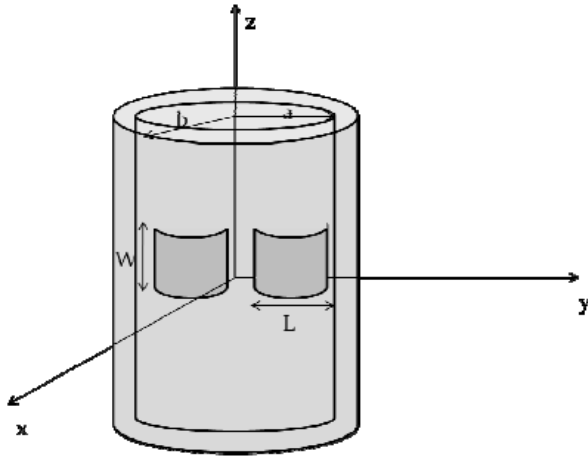


Fig 2: Two element array in HH-Plane on curved surface

Where, the superscript denotes the port quantities. Z11 stands for input impedance of patch-1 with patch -2 open-circuited, while, Z12 and Z21 stand for mutual impedance of patches. Z22 stands for input impedance of patch-2 with patch open-circuited.

Since measurement of voltages and currents at microwave frequencies is difficult, a scattering matrix related to the direct measurement of incident, reflected, and transmitted waves is used to describe the multiport network problem completely. Scattering matrix [S] can be evaluated as.

## VII. RESULTS

An array of two rectangular patches has been formed on cylindrical surface in E and H-plane. The microstrip patch has been designed for the S-band frequency ranges (3GHz in this case). It is important to note that microstrip patch antenna working on this frequency range finds application in weather radar, surface ship radar, and some communications satellites.

The design flow for the single patch dimensions, using the cavity model approach as described in chapter 3 is as follows:

- Fr, frequency of operation = 3 GHz
- Er, relative permittivity of substrate material= 2.32
- h, height of substrate = 0.159 cm
- Calculated length and width of patch are:
- L, length of patch = 3.2 cm
- W, width of patch = 3.8 cm
- The dominant mode is thus TM01.

The results have been obtained using MATLAB-2010a. This chapter includes plots of basis function, behavior of Green's function, behavior of integrand, surface current, E and H-plane radiation patterns and mutual coupling coefficient (S12) plots.

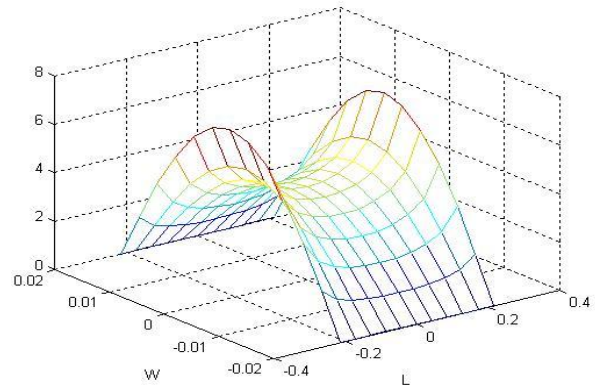


Fig 3(a): Patch Surface Current Density obtained from MoM application assuming patch current variation only in z-direction

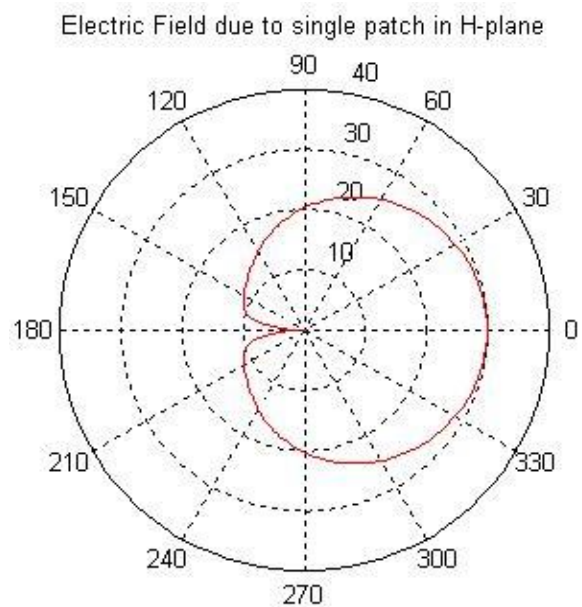


Fig 3 (b): H-plane radiation pattern for single patch

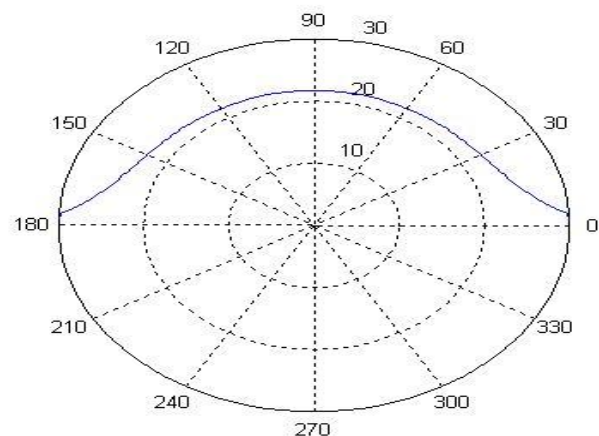


Fig 3 (c): E-plane radiation pattern for single patch

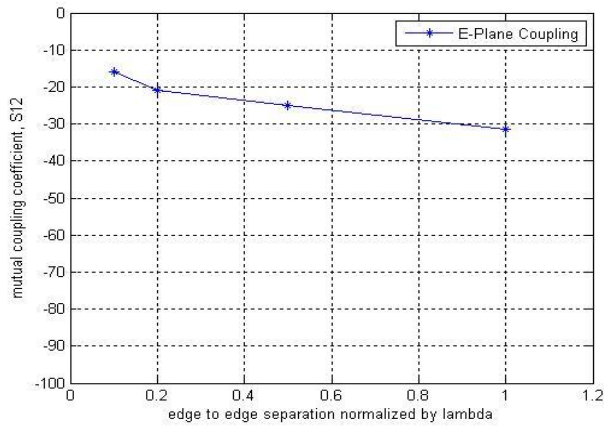


Fig 3 (d): Mutual coupling plots in E-plane

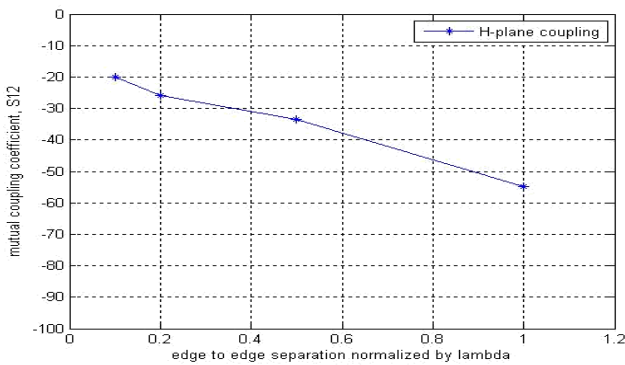


Fig 3 (e): Mutual coupling plots in H-plane

### VIII. CONCLUSIONS

The radiation pattern for single patch for E-plane and H-plane has been obtained. Mutual coupling coefficient S12 for different elemental spacing in E and H-plane is plotted. Results show good agreement with that in available literatures. The results show that with the increase in elemental spacing in terms of lambda mutual coupling decreases, which is more prominent in H-plane.

In this work, only mutual coupling coefficients for four edge spacing have been calculated. The accuracy can be further improved by including more points in between. The results need to be verified with commercially available software or by practical means.

The same analysis can also be carried out for a larger array which is generally used for practical applications.

### IX. ACKNOWLEDGEMENTS

All the Authors are thankful to the Director-Principal, and the management for their support in providing the necessary software and permission to publish this paper.

### REFERENCES

- [1] Ramesh Garg, Prakash Bhartia, Inder Bahl, Apisak Ittipiboon, "Microstrip Antenna Design Handbook," Artech House, 2000.
- [2] Constantine A. Balanis, "Antenna Theory Analysis and Design," Wiley Interscience, 2005.
- [3] I. J. Bahl and P. Bhartia, "Microstrip Antennas," Artech House, Dedham, MA, 1980.
- [4] Kin-Lu Wong, "Design of Non-planar Microstrip Antennas and Transmission Lines," John Wiley & Sons, Inc., 1999.
- [5] Sean M. Duffy, "An Enhanced Bandwidth Design Technique for Electromagnetically Coupled Microstrip Antennas," IEEE

Transactions on Antennas and Propagation, Vol. 48, No. 2, February 2000.

- [6] J. R James and P. S Hall, "Handbook of Microstrip Antennas," Peter Peregrinus Ltd., London, United Kingdom 1989.
- [7] S. Karan, V. B. Erturk, and A. Altintas, "Closed-Form Green's Function Representations in Cylindrically Stratified Media for Method of Moments Applications," IEEE Transactions on Antennas and Propagation, Vol. 57, no. 4, April 2009.
- [8] Constantine A. Balanis, "Advanced Engineering Electromagnetics," John Wiley & Sons, 1989.
- [9] Lars Josefsson and Patrik Persson, "Conformal Array Antenna Theory and Design," IEEE Antennas and Propagation Society, Wiley Int. Publication, 2006.